Driving a Ballbot Wheelchair with Hands-Free Torso Control

Seung Yun Song†
Mechanical Science and Engineering
The University of Illinois at Urbana-Champaign
Urbana IL USA ssong47@illinois.edu

Nadja Marin
Mechanical Science and Engineering
The University of Illinois at Urbana-Champaign
Urbana IL USA nadjam2@illinois.edu

Chenzhang Xiao
Mechanical Science and Engineering
The University of Illinois at Urbana-Champaign
Urbana IL USA cxiao3@illinois.edu

Mahshid Mansouri
Mechanical Science and Engineering
The University of Illinois at Urbana-Champaign
Urbana IL USA mm64@illinois.edu

Joao Ramos
Mechanical Science and Engineering
The University of Illinois at Urbana-Champaign
Urbana IL USA jlramos@illinois.edu

Yu Chen
Mechanical Science and Engineering
The University of Illinois at Urbana-Champaign
Urbana IL USA yuc6@illinois.edu

Adam W. Bleakney
Applied Health Sciences & Beckman Institute
The University of Illinois at Urbana-Champaign
Urbana IL USA bleakney@illinois.edu

Deana C. McDonagh
Beckman Institute
The University of Illinois at Urbana-Champaign
Urbana IL USA mcdonagh@illinois.edu

William R. Norris
Industrial and Enterprise Systems Engineering
The University of Illinois at Urbana-Champaign
Urbana IL USA wrnorris@illinois.edu

Jeannette R. Elliott
Disability Resources and Educational Services
The University of Illinois at Urbana-Champaign
Urbana IL USA elliott3@illinois.edu

Patricia B. Malik
Disability Resources and Educational Services
The University of Illinois at Urbana-Champaign
Urbana IL USA pmalik@illinois.edu

Elizabeth T. Hsiao-Wecksler
Mechanical Science and Engineering
The University of Illinois at Urbana-Champaign
Urbana IL USA ethw@illinois.edu

ABSTRACT

A novel wheelchair called PURE (Personalized Unique Rolling Experience) that uses hands-free (HF) torso lean-to-steer control has been developed for manual wheelchair users (mWCUs). PURE addresses limitations of current wheelchairs, such as the inability to use both hands for life experiences instead of propulsion. PURE uses a ball-based robot drivetrain to offer a compact, self-balancing, omnidirectional mobile device. A custom sensor system converts rider torso motions into direction and speed commands to control PURE, which is especially useful if a rider has minimal torso range of motion. We explored whether PURE's HF control performed as well as a traditional joystick (JS) human-robot interface and mWCUs, performed as well as able-bodied users (ABUs). 10 mWCUs and 10 ABUs were trained and tested to drive PURE through courses replicating indoor settings. Each participant adjusted ride sensitivity settings for both HF and JS control. Repeated-measures MANOVA tests suggested that the number of collisions, completion time, NASA TLX scores except physical demand, and index of performances were similar for HF and JS control and between mWCUs and ABUs for all sections. This suggests that PURE is effective for controlling this new omnidirectional wheelchair by only using torso motion thus leaving both hands to be used for other tasks during propulsion.

†Corresponding Author

HRI '24, March 11–14, 2024, Boulder, CO, USA.

ACM ISBN 979-8-4007-0322-5/24/03.
https://doi.org/10.1145/3610977.3634957

CCS CONCEPTS

• Human-centered computing • Human Computer Interaction

KEYWORDS

Self-balancing; Mobility Device; Lean-to-Steer; Mobile Robot

ACM Reference format:

Seung Yun Song, Nadja Marin, Chenzhang Xiao, Mahshid Mansouri, Joao Ramos, Yu Chen, Adam W. Bleakney, Deana C. McDonagh, William R. Norris, Jeannette R. Elliott, Patricia B. Malik, Elizabeth T. Hsiao-Wecksler. 2024. Driving a Ballbot Wheelchair with Hands-Free Torso Control. In *Proceedings of 2024 ACM/IEEE International Conference on Human-Robot Interaction (HRI '24), March 11-14, 2024, Boulder, Colorado, USA.* ACM, New York, NY, USA, 9 pages. https://doi.org/10.1145/ 3610977.3634957

Figure 1. Novel wheelchair (PURE) uses torso motions for (a) hands-free control to move omnidirectionally: (b) forward-backward, (c) sideways, and (d) spin in place.

1 INTRODUCTION

In the US alone, over 6.8 M people use manual or powered wheelchairs [1]. These traditional wheelchairs have limitations such as the inability to use both hands while moving, large footprints, high risks for shoulder injuries for manual wheelchair users [2], and large bulk and weight of powered wheelchairs. Some new mobility devices are addressing these limitations.

A promising approach used self-balancing technology [3]–[8]. Self-balancing wheelchairs are human rideable dynamically stable mobile robots that are compact in size. These devices operate like a Segway and can be represented as the classic wheeled inverted pendulum model that maintains its balance by monitoring the system's kinematics and strategically actuating the wheels [9]. These devices require the user to lean their body, offsetting the system's center of mass (COM), to propel or brake [8]. However, these two wheeled self-balancing wheelchairs lack maneuverability and practicality, especially in tight spaces, due to their heavy weight (75kg), large size (W, L = 650mm, 740mm), incapability of moving laterally and customizing the ride sensitivity. Some even have joysticks or levers for steering, demanding the use of hands during maneuvers. The Honda UNI-ONE [3], a hands-free mobility device, is a promising solution. However, the UNI-ONE requires the user to switch between different drive modes (e.g., steer vs. slide) via a smartphone application, requiring the use of hands. Also, there were no test reports on wheelchair users riding the UNI-ONE. Thus, in this study, a novel personal mobility device called PURE (Personalized Unique Rolling Experience) that addresses these limitations was developed and tested on wheelchair users.

1.1. PURE Overview

PURE's drivetrain uses a ball-based robot (ballbot) concept (Figure 1(a)) [8]. A ballbot is a dynamically stable mobile robot that balances on a single spherical wheel, i.e., ball. PURE's direction and speed can be controlled with signals generated either with a 3-axis joystick or more uniquely using hands-free (HF) control based on torso motions. In the HF control, the rider drives PURE by 1) leaning the torso forward-backward to steer PURE longitudinally (Figure 1 (b)), 2) leaning the torso right-left to slide PURE laterally (Figure 1 (c)), 3) twisting the torso to spin PURE about the vertical axis (Figure 1 (d)), and 4) performing combinations of the three actions. Thus, PURE can move in non-cardinal directions (e.g., diagonal) by the user leaning diagonally.

PURE's has a minimal physical footprint (530×607 mm) as well as a seat height comparable to a traditional manual wheelchair (mWC) (Figure 2(a)). PURE's footprint is smaller than a typical mWC due to the compact ballbot-based design. Additionally, PURE's seat height followed a typical seat height of a traditional mWC to provide easy transfer and comfortable ride height.

PURE's design consisted of upper and lower parts (Figure 2(b)). The upper part comprises a user-interface (UI) control panel, joystick, and Torso-dynamics Estimation System (TES). The lower part comprises of PURE's ballbot drivetrain, which consists of a ball, three omniwheels (each actuated by a motor), and a safety ring.

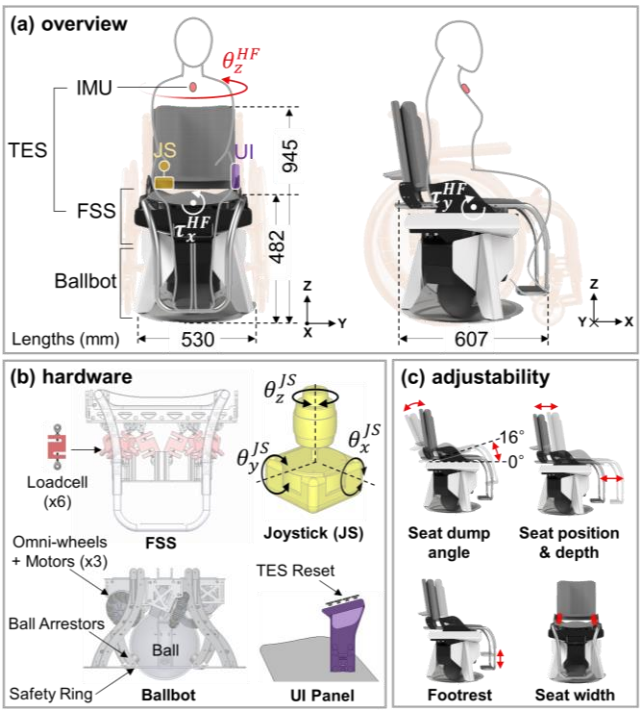

Figure 2. PURE's design hardware overview and key features. A validated sensor system that quantified rider's torso motions in terms of kinetic and kinematic signals is utilized to provide these tunable reference signals [11].

The ball is controlled omnidirectionally by strategically powering the three motors in various directions and speeds [8], [10]. The seat is lightweight and adjustable to accommodate different riders (Figure 2(c)). The seat width, depth, dump angle, backrest height, and footrest height can be altered. The seat fore/aft position is adjusted to align the rider's COM vertically to the ball center.

Some riders may not have enough torso range of motion to offset the system's COM to move or stop, while others may prefer faster or slower system responses to torso movement. To address these issues, PURE provided adjustable ride sensitivity (i.e., device accelerates or decelerates faster for a small torso lean) to fit a rider's ability or preference. To adjust the ride sensitivity, PURE used the TES to quantify the rider's torso motions to provide tunable reference signals for the ballbot controller to track [11].

The TES consisted of a custom instrumented seat (Force Sensing Seat – FSS) and an inertial measurement unit (IMU) (Figure 2(a,b)). The FSS estimated the contact forces, torques, and center of pressures between the rider and the seat to provide reference signals to control the ballbot's translational speeds along the x-, y-axes[11]. A 9-axis IMU was attached to the rider's upper chest to estimate the torso twist angle about the vertical z-axis to command the PURE's rotational speed about the z-axis (Figure 2(a)).

The PURE controller system consisted of a translational and a spin controller to govern the 2D translational maneuvers in the x-, y-axis and rotational maneuvers about the z-axis, respectively (Figure 3) [8], [10]. For the translational and spin control, PURE

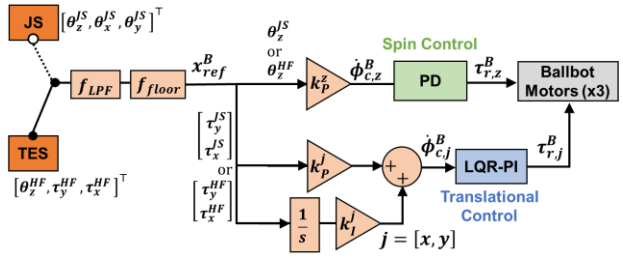

Figure 3. PURE controller and preprocessing of HRI signals.

utilized a cascaded LQR-PI controller and PD controller, respectively. Translational and spin command speeds of the ball ($\dot{\phi}^B_{c,x}, \dot{\phi}^B_{c,y}, \dot{\phi}^B_{c,z}$) generated from either the TES or JS readings are input to the controllers. The raw TES and JS signals are preprocessed before being input into the PURE's controllers to provide stable reference signals (Figure 3) [12]. The output signals from the controllers are used as ball torque reference signals ($\boldsymbol{\tau}^{\boldsymbol{B}}_{\boldsymbol{r,j}}$, $\boldsymbol{\tau}^{\boldsymbol{B}}_{\boldsymbol{r,z}}$) to command the ballbot motors. There was minimal and unnoticeable time delay between the user's input and PURE's motion since the LQR controller was optimized for the user's weight and estimated inertia.

For the translational controller, and for HF control, a proportional and integral terms are combined to compute $\dot{\phi}^B_{c,j}$, where k^j_P, k^j_I, $j \in [x, y]$, are tunable gain parameters to adjust PURE's ride sensitivities (Figure 3). The proportional term is analogous to an automobile's accelerator pedal that governs the mapping between the magnitude of torso lean and the ballbot's translational speed. A higher k^j_P allows a slight leaning of torso to quickly accelerate PURE, which benefits riders with low torso mobility. The integral term serves like an automobile's cruise control that enables the rider to maintain a constant speed without torso leaning. The rider can lean forward to accelerate PURE and then lean back to neutral position to maintain a constant speed, proportional to k^j_I. To turn off the "cruise control", the rider can lean backwards. The integral term reduces the rider's physical effort since PURE can move without constant torso lean. For JS control, $\dot{\phi}^B_{c,j}$ was determined only by the proportional term ($k^j_P \theta^{JS}_j$). The integral term is unnecessary since joysticks do not need much physical effort.

PURE used the spin controller for changing its heading angle (Figure 3). For HF control, the IMU's yaw angle (θ^{HF}_z), which represents the rider's torso twist angle about the vertical axis, is used as the reference signal. For JS control, the joystick's yaw angle (θ^{JS}_z) is used as the reference signal. The spinning sensitivities can be adjusted using tunable parameters for HF ($k^{z,HF}_P$) and JS ($k^{z,JS}_P$) control. The value of k^z_P depends on the sign of θ^{HF}_z to allow different sensitivities for spinning clockwise or counterclockwise which assists mWCUs with asymmetric torso range of motion. Higher $k^{z,HF}_P$ increases the sensitivity, allowing riders with low torso mobility to easily change PURE's heading angle. Likewise, higher $k^{z,JS}_P$ increases the joystick's sensitivity for rotating PURE.

1.2. Study Goals

Previously, a virtual-reality simulation study was conducted to investigate the feasibility of using the TES for hands-free control of a virtual PURE ballbot [12]. Ten mWCUs and ten able-bodied users (ABUs) navigated the virtual PURE through a virtual-reality course. Repeated measures MANOVA tests assessed performance metrics representing efficiency (i.e., number of collisions), effectiveness (i.e., completion time), comfort (i.e., NASA TLX scores), and robustness (i.e., index of performance). Statistical results demonstrated that the HF control performed as well as JS control, and mWCUs performed similarly to ABUs. However, the virtual test setup could not completely replicate the real-world dynamics of the PURE-rider system or provide participants with any proprioceptive feedback from the movement of a real PURE. Thus, a study evaluating the HRI performances of HF and JS control while driving a physical PURE was needed. The goals of this study were to determine 1) if HF control performed similarly to JS control, and 2) if mWCUs and ABUs could ride the physical PURE with similar performance using HF or JS control. Participants drove PURE using HF and JS control in a challenging indoor course designed to replicate various indoor environments.

2 METHODS

2.1. Participant Demographics

Twenty young age- and gender-matched ABU and mWCU participants were tested (Table 1). For all participants, the inclusion/exclusion criteria were that they 1) were 18 to 35 years old, 2) could comfortably manipulate the joystick using fingers, 3) had no recent injury to their dominant arm or hand within the past 3 months, 4) weighed < 80 kg, and 5) had no visual impairment with visual correction. For ABUs, additional inclusion-exclusion criteria were that they had no history of neck, arm, or back related surgery and disorders. For mWCUs, the additional inclusion-exclusion criteria were that they 1) had at least minimal trunk control with sensation to at least the level of the xyphoid process and 2) were experienced manual wheelchair users who used a wheelchair daily for a minimum of one year and at least 50% of waking hours. This study was conducted at the university campus and approved by the university's Institutional Review Board (IRB #22891), and informed consent was received.

Basic biometric information was collected for all participants (Table 1). The upper-body COM height, defined as the vertical distance from the seat surface to participant's xyphoid, was recorded since the PURE's dynamics were affected by the rider's COM location. Likewise, self-reported total mass with shoes and height without shoes were recorded.

Torso mobility was quantitatively characterized by the torso range of motions (ROMs) and torso asymmetry in different planes (Table 1). These torso ROMs ($\left[\theta^{ROM}_x, \theta^{ROM}_y, \theta^{ROM}_z\right]^T$) were calculated by collecting the IMU data while the participant performed predefined torso movements. The torso ROMs were computed for torso leaning in the frontal plane with rotation about the rider's x-axis (θ^{ROM}_x) and the sagittal plane with rotation

TABLE 1. PARTICIPANT DEMOGRAPHICS DATA

		ABU	mWCU
N (Male: Female)		10 (5:5)	10 (5:5)
Age (years)		[a]24.6 (3.2)	26.0 (5.3)
Height without shoes (m)		1.69 (0.06)	1.63 (0.11)
Upper-body COM Height (m)		0.39 (0.03)	0.37 (0.06)
Total Mass with shoes (kg)		62.0 (11.3)	53.8 (11.4)
Torso ROM (˚)	θ_x^{ROM}	78.0 (25.4)	47.7 (16.1)
	θ_y^{ROM}	97.2 (25.2)	39.9 (17.3)
	θ_z^{ROM}	115.5 (16.0)	62.9 (32.7)
Torso Asymmetry (%)	ζ_x	8.2 (6.1)	17.2 (17.6)
	ζ_y	16.0 (19.0)	24.9 (11.4)
	ζ_z	5.4 (6.2)	21.3 (21.2)
Joystick Sensitivities	[b]$k_P^{x,JS}$	20.1 (5.7)	21.9 (5.9)
	[b]$k_P^{y,JS}$	8.9 (1.6)	13.8 (5.9)
	[b]$k_P^{z,JS}$	5.7 (1.1)	8.4 (9.4)
Hands-Free Sensitivities	[c]$k_P^{x,HF}$	100.0 (9.4)	167.0 (67.5)
	[d]$k_I^{x,HF}$	58.0 (13.0)	99.5 (44.5)
	[c]$k_P^{y,HF}$	0.0 (0.0)	0.0 (0.0)
	[e]$k_{P,CW}^{z,HF}$	260.0 (137.0)	254.0 (110.3)
	[e]$k_{P,CCW}^{z,HF}$	240.0 (132.9)	281.0 (203.5)

[a]Average (Standard Error)

[b]$k_P^{x,JS}, k_P^{y,JS}, k_P^{z,JS}$: proportional terms governing PURE's sensitivity in x-, y-, z-axis for a given joystick input in JS control

[c]$k_P^{x,HF}, k_P^{y,HF}$: proportional terms governing PURE's sensitivity about x-,y-axis for a given torso lean in HF control

[d]$k_I^{x,HF}$: integral term governing cruise control in HF control along x-axis

[e]$k_{P,CW}^{z,HF}, k_{P,CCW}^{z,HF}$: proportional terms governing PURE's sensitivity about z-axis for a given torso twist in clock & counter-clockwise direction in HF control

about the y-axis (θ_y^{ROM}), and torso twisting in the transverse plane with rotation about the z-axis (θ_z^{ROM}). Torso asymmetry was also computed from the IMU data. Participants with spinal deformities were reported to display asymmetric torso mobility [13]. Thus, a metric (ζ_u) was introduced to represent the degree of asymmetry for torso leaning in the sagittal (ζ_y) and frontal (ζ_x) planes and twisting in the transverse plane (ζ_z). Equations on the torso ROM and asymmetry are in Appendix 1.

mWCU's underlying disorders and their level of mWC experience were collected to understand each participant's degree of torso mobility (Appendix 2). Since most were collegiate para-athletes, the athletic ratings for their respective sports were collected. Also, previous experience using the JS and HF control as well as self-balancing devices and balance-related sports were collected. Understanding these past experiences was essential to ensure both groups had similar level of proficiency for using JS and HF control to eliminate any confounding variables affecting the navigational performance except for the type of HRIs or participant groups.

Tunable HRI sensitivities (Table 1) and seat settings (Appendix 2) were recorded to understand the differences of ride sensitivity and seat preferences.

2.2. Training and Test Course

A training and test course were devised for training and evaluation purposes. The two courses were designed differently to prevent the participants from memorizing the sections and for fair assessment. Both courses consisted of various sections (e.g., straight, slide, spin, turn, bathroom, static obstacles, and moving obstacles) (Figure 4). Straight, turn, and slide section had various hallway widths to introduce multiple levels of difficulty. The dimensions and layout of the sections followed the U.S. building and Americans with Disabilities Act (ADA) codes [14]. The simulated hallways boundaries were indicated using differently colored tapes. All sections (except for bathroom and static obstacle) contained various difficulty levels to test the participants in different indoor scenarios. For static obstacles, 2D paper cutouts from foam core boards were used. For moving obstacles, a moving image from a projector mounted above the course was utilized.

The training course consisted of six sections: spin, straight, slide, static obstacles, and moving obstacles (Figure 5). The goals were to assist the participants in familiarizing themselves with driving PURE and personalize the sensitivities for the JS and HF control before the test course. The participants had to finish each section of the training course successfully (i.e., perform the given task without crossing the boundaries or colliding with the obstacles) before moving on to the next section. A collision was defined as the instance when any part of the PURE's safety ring went over the taped boundaries or obstacles. During each section, adjustments were made to the tunable parameters for the HF (i.e., $[k_P^{j,HF}, k_I^{j,HF}, k_P^{z,HF}]$) or JS control (i.e., $[k_P^{j,JS}, k_P^{z,JS}]$) by periodically asking the rider for feedback. All tunable parameters started from zero and were incrementally increased until the rider was satisfied. More training protocol is detailed in Appendix 3.

The objective of the test course was to evaluate the performances of HF and JS control thoroughly and objectively by imposing different challenges for each section. The test course consisted of four laps with different layouts and difficulties (Figure 6). Each lap consisted of multiple sections. The first lap was composed of five sections: Wide (W) straight, W left turn, bathroom, W right turn, left turn, and N right turn sections. The final lap contained four sections: Extra narrow (EN) straight, EN left turn, EN right turn, and moving obstacles (slow (S), medium (M), fast (F)) sections.

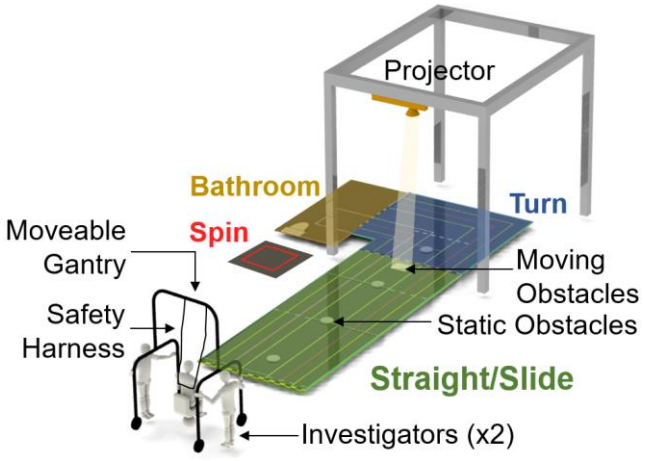

Figure 4. Overall course was divided into various sections replicating real-life indoor environments.

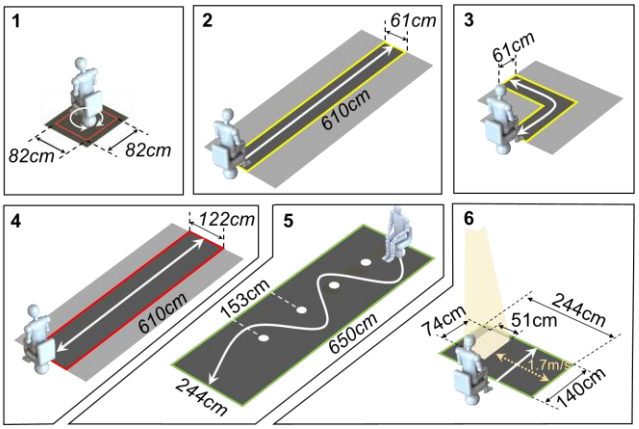

Figure 5. The training course consisted of 1) spin, 2) straight, 3) turns, 4) slide, 5) static obstacles, and 6) moving obstacle sections. The safety gantry was not shown for visual purposes.

The first lap was the easiest among the four laps due to ample free space, and the consecutive laps became more difficult due to narrower paths and more complex obstacles. Each section began with the participant positioned in the middle of the starting line, and an investigator verbally notified the participant when to start.

The straight and turn section consisted of four paths with different widths: wide (W), medium (M), narrow (N), and extremely narrow (EN) (Figure 7). The goal of the straight and turn sections were to navigate through a linear (610 cm) path and L-shaped (305 cm × 305 cm) path, respectively, without crossing the taped boundaries. These sections tested the ability of driving in a straight line and steering at various difficulties. The W, M, and N paths were used to simulate a large academic/public building (e.g., hospital) hallway width, average residential hallway width, and narrow residential hallway width, respectively. The EN path was a significantly more challenging path than the previous three since it allowed only 4 cm of space between PURE and the boundaries on each side. The EN path width was narrower than the minimum allowable hallway width (92 cm) suggested by U.S. building code. The EN path was added

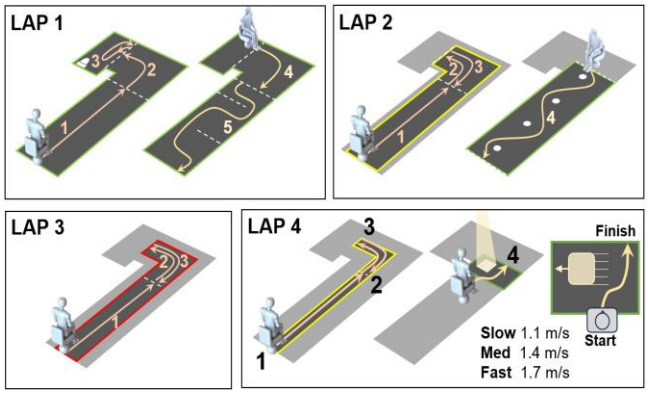

Figure 6. The testing course consisted of four laps with various layouts and difficulties (gantry not shown for visibility purposes). White dashed lines define start-end of sections.

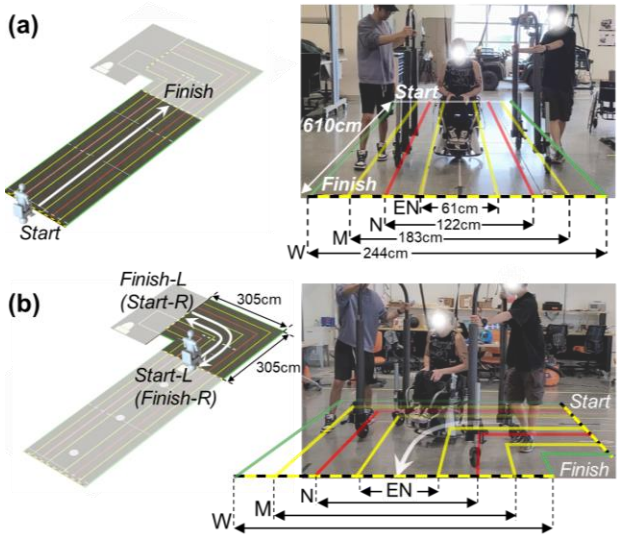

Figure 7. (a) Straight and (b) turns consisted of extreme narrow (EN), narrow (N), medium (M), and wide (W) widths.

to provide sufficient level of difficulty to rigorously test the performances of HF and JS control since pilot test participants were able to navigate through the N to W paths too effortlessly. For testing, the participant was told to go through all four paths, EN to W. The remaining sections are explained in Appendix 4.

2.3. Protocol

Prior to testing, participant information was collected, and the PURE's hardware was adjusted for each rider. Hardware adjustments included modifications of the seat, backrest, and footrest. For mWCUs, PURE's seat adjustments closely followed the dimensions of their current mWC, and their personal seat cushion was used on PURE to maximize comfort. For ABUs, incremental adjustments were made until the participants expressed comfort. The IMU was attached to the participant's manubrium using double-sided adhesives. Each participant's torso ROMs were computed by collecting the IMU data while the participant sat on PURE while stable and the motors were off and performed predefined the torso movements explained in [11].

For added safety, the rider wore a safety harness tethered to a movable gantry system (Figure 4, Figure 7). The safety harness straps were long enough to allow unobstructed navigation while short enough to safeguard the rider from hitting the floor in the unlikely event of a fall. Two investigators manually moved the gantry system, following the rider to remove any tension in the harness. A third investigator remotely monitored the safety of PURE and disabled the PURE in emergency cases.

For both courses, the participant was instructed to navigate through each section without colliding into obstacles or boundaries at their comfortably fast speed. The participant was first trained by going through a predefined training course once each: 1) using the JS control, or 2) the HF control (training order was randomized). After training, the participant's navigation performance was evaluated on a test course. Like the training course, the test course was completed once each using the HF and

JS control, in randomized order. For every section, the number of collisions (N_c), successful completion time (t_{sc}), and video footages were recorded. An investigator visually monitored and counted N_c. t_{sc} was defined as the duration from the verbal start cue to the time when the PURE's safety ring touched the finish line. Only the duration with no collisions (i.e., the last attempt) was recorded. The participant had to start at the beginning of a section after every collision. After finishing each section, the participant was asked to reposition at the starting line of the next section.

Immediately after completing the experiment, the participant took the NASA Task Load indeX (NASA TLX) survey [15] and a multiple-choice question. The survey was given to each participant to subjectively evaluate the level of comfort for HF and JS control. The NASA TLX is a widely used tool for measuring subjective mental and physical workload for various human-robot interfaces [15]. The six NASA TLX scores are calculated by having the participant subjectively score each interface in terms of mental demand, physical demand, temporal demand, effort, performance, and frustration [15]. Each score ranged from 0 to 100-points with 5-point steps, where a lower number indicated more comfort (including performance). In addition, a multiple-choice question was administered: "If you were to use the hands-free method in your daily life, how long do you think you would use the device before truly becoming tired? (0 – 10 min, 10 – 30 min, 30 – 60 min, > 60 min)" was asked from each participant to understand the level of physical fatigue of using the HF control.

2.4. Data Analysis

The performances of each HRI were evaluated using four attributes quantified by objective and subjective metrics. These four attributes were effectiveness, efficiency, comfort, and robustness since these attributes are the most relevant information for evaluating the performance of human-robot interfaces in navigation and teleoperation tasks [16]–[19]. Effectiveness (i.e., how well the task is completed) and efficiency (i.e., how quickly the task is completed) were described by N_c and t_{sc}, respectively [16]–[19]. Comfort (i.e., how easy the task is to complete mentally and physically) was quantified using the six NASA TLX [15] scores. Robustness (i.e., how sensitive the HRI performance is to various difficulty levels of the task) was quantified using an index of performance (IOP) [20]–[22]. The index of performance (IOP) is derived from the Accot-Zhai Steering Law, a predictive model for describing the changes in task performances (e.g., $t_{sc}$for navigating through a course with a fixed length) across different levels of task difficulties (e.g., EN to W widths). The IOP is a widely used metric for quantifying the performance and robustness in navigation tasks for human-computer interaction. More details can be found in [20]–[22]. Higher values of IOP for a given interface indicate more robustness, i.e., similar performance (e.g., t_{sc}) even for difficult course sections (e.g., narrower path width). This study computed IOP for straights and turns (average of left and right turns) for HF and JS control. Thus, a total of eight IOPs (= 2 course types (i.e., straight, turn) × 2 HRIs × 2 participant groups) were computed.

2.5. Statistical Analysis

Repeated-measures multivariate ANOVA (MANOVA) tests were performed using IBM SPSS (SPSS Statistics Version 28.0.1, IBM Corp, USA) to determine 1) if the HF control performed as well as the JS control, and 2) if mWCUs performed as well as ABUs. The performance was assessed using N_c, t_{sc}, NASA TLX scores, and IOPs. Since 1) N_c and t_{sc} were computed for each section and 2) NASA TLX scores, $IOP_{straight}$, IOP_{turns} were calculated after going through all sections, we performed two separate MANOVA tests. However, before the two tests, four MANOVA tests were conducted to determine if the N_c, t_{sc} data of each of the four section types (i.e., straights, turns, slides, moving obstacles) with three difficulties (i.e., widths or speeds) could be combined across all difficulties into four sections by averaging the N_c, t_{sc} data for the sections with three widths or three speeds. The consolidation could improve the power of the two MANOVA tests by reducing the number of sections (details in Appendix 5). The four MANOVA consolidation tests revealed that there were no significant differences between the two interfaces or participant groups for the four sections (i.e., straights, turns, slides, moving obstacles) with three widths or speeds. Thus, these four sections were consolidated. As a result, the consequential MANOVA tests for N_c and t_{sc} were conducted using eight sections. Thus, two MANOVA tests were performed: 1) a three-way MANOVA {2 (interface: HF, JS) × 2 (group: ABUs, mWCUs) × 8 (sections: averaged straights, averaged turns, averaged slides, averaged moving obstacles, EN straight, EN turns, static obstacles, bathroom stall)} with two dependent variables (i.e., N_c, t_{sc}), and 2) a two-way MANOVA {2 (interface: HF, JS) × 2 (group: ABUs, mWCUs)} with eight dependent variables (i.e., six NASA TLX scores, $IOP_{straight}$, IOP_{turns}). Follow-up univariate ANOVAs were performed on significant dependent variables for each MANOVA; these were followed by LSD post-hoc comparisons where appropriate. Significance levels were 0.05 for all analyses.

3 RESULTS

The MANOVA tests revealed that there were no statistically significant differences between the HF and JS control for all performance metrics (i.e., N_c, t_{sc}, six NASA TLX Scores, $IOP_{straight}$, IOP_{turns}) except for the physical demand score from the NASA TLX survey ($p < 0.001$ using univariate ANOVA) (Figure 8). MANOVA tests suggested that there were no statistically significant differences between the mWCUs and ABUs for all performance metrics (Figure 8). mWCUs had similar N_c, t_{sc}, NASA TLX scores (except for physical demand), and IOPs as ABUs for the entire course. No statistically significant interaction effects were observed. N_c, t_{sc} varied based on the difficulty and type of the section (Figure 8). N_c was highest for the section with fast moving obstacles. Little to no collisions were observed for all interfaces or participant groups for N to W straights, N to W turns, N to W slides, bathrooms, and static obstacle sections. For EN turns and EN straights, the N_c increased for all interfaces and participant groups. The moving obstacle section, especially for the fast-moving obstacles, demonstrated higher N_c than other

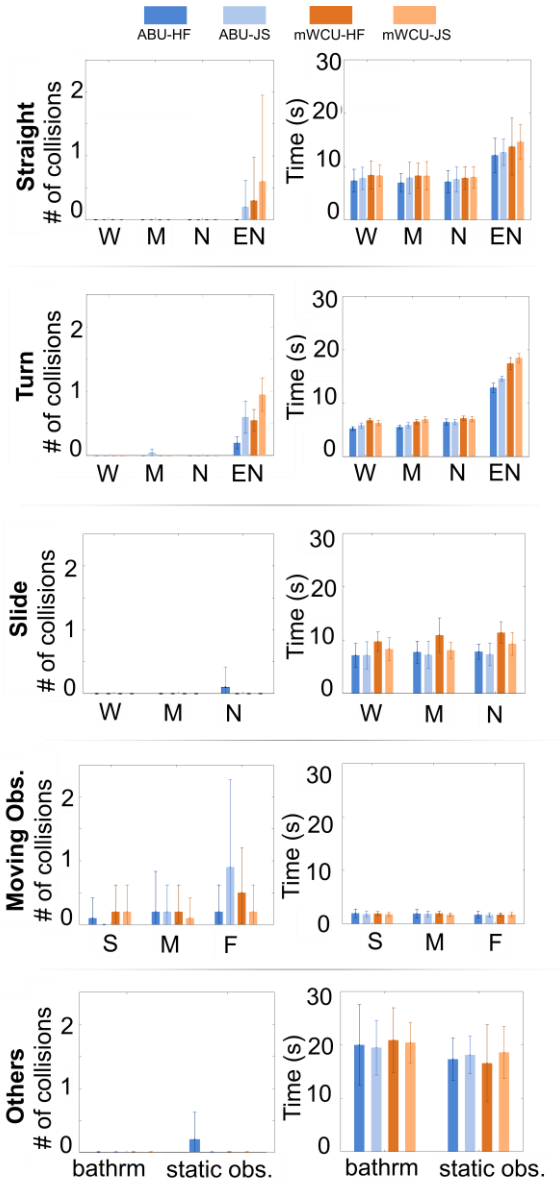

Figure 8. Average and standard errors of the number of collisions and successful completion time for various course sections.

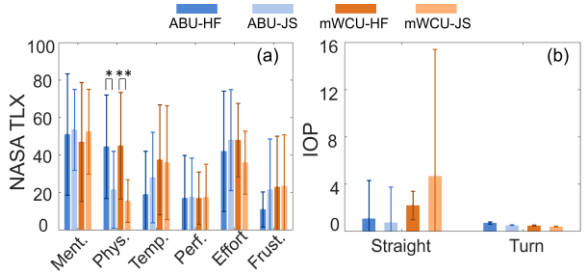

Figure 9. Average and standard errors of (a) NASA TLX scores for mental (Ment.), Physical (Phys.), Temporal (Temp.), Performance (Perf.), Effort, Frustration (Frust.) (b) Index of Performance (IOP) for straight and turn.

sections for all interfaces and participant groups. t_{sc} was the highest for bathrooms and static obstacle courses, followed by EN turns, EN straights, N to W turns, N to W straights, slides, and moving obstacles. However, the N_c, t_{sc} were similar between HF and JS control for mWCUs and ABUs, even for the difficult EN and fast-moving obstacle sections.

The mWCUs and ABUs gave similar ratings for the HF and JS control on the NASA TLX survey for all categories except for the physical demand score (Figure 9(a)). For the physical demand score, both participant groups rated the HF control higher than the JS.

For robustness, the IOPs were similar for the straights and turns for all interfaces and participant groups (Figure 9(b)). The mWCUs using the JS control displayed higher IOP and standard errors.

For the post-study questions assessing the level of fatigue, 50%, 30%, and 20% of the ABUs expressed they could use the HF control longer than 1 hour, 30 min – 1 hour, and 10 min – 30 min, respectively. 90%, 10%, and 0% of the mWCUs expressed they could use the HF control for longer than 1 hour, 30 min – 1 hour, and 10 min – 30 min, respectively.

4 DISCUSSIONS

The proposed HF control performed similarly to the commonly used JS control, and the mWCUs performed closely to the ABUs for driving PURE through a challenging indoor course complying with the US building and ADA standards (Figure 8, Figure 9). The tested mWCUs exhibited significantly smaller torso ROM and higher torso asymmetry than ABUs in all three planes (Table 1).

The torso-based HF control was as effective and efficient as JS control, and mWCUs navigated PURE as effectively and efficiently as ABUs. The N_c, t_{sc} were similar between the two interfaces and participant groups even for challenging sections with very little free space and obstacles moving at fast walking speeds (Figure 8). In some sections such as EN straights/turns and moving obstacles, the HF control was surprisingly more effective and efficient than JS.

For mWCUs and ABUs, the HF and JS control were equally comfortable to use (Figure 9(a)). ABUs even preferred the HF over JS control in terms of temporal demand and frustration scores from the NASA TLX survey. While the HF control scored higher than the JS control on NASA TLX's physical demand category, most participants (70%) reported that they could continuously ride PURE using the HF control for longer than an hour without getting fatigued. Interestingly, a greater majority of mWCUs (90%) than the ABUs (50%) expressed they could use the HF control for longer than an hour. In our study, the participants rode PURE using HF control for a long duration (1~2 hours), and no participants expressed any significant physical fatigue. Also, some level of physical demand may be beneficial by motivating mWCUs to engage their core muscles, mitigating risks of pressure ulcers [13].

The HF control was as robust as the JS control, indicating that the HF control was effective regardless of the path difficulty (Figure 9(b)). Also, the mWCUs navigated PURE as robustly as

ABUs, demonstrating that users with less torso function could adapt to courses with more difficulty. The robustness was quantified using index of performance, a well-established metric for assessing human-robot interfaces.

PURE's hardware adjustability was critical to accommodate the diverse riders. While the biometrics of tested ABUs and mWCUs were similar, the preferred seat dimensions greatly varied between the two groups (Table A.2.3). Others have reported similar findings [23]. Customization of the seat was needed for a comfortable user experience, which affects their performances with the HF control. For example, a backrest that was too high obstructed the rider from comfortably leaning backwards or twisting. These seat dimensions play critical roles that impact daily lives in practical settings [24].

The tunable parameters of the HF and JS sensitivity control was vital to satisfy each rider's preference and mobility. These parameters greatly varied between and within participant groups (Table 1). For the HF control, k_P^x and k_I^x were higher for the mWCUs, suggesting that the mWCUs preferred more sensitive ride behavior in the forward/backwards direction to compensate for their lack of torso mobility. These parameters also varied greatly among mWCUs, suggesting that each mWCU desired different ride sensitivities due to large variations in their torso mobilities. Also, the mWCUs preferred the use of the cruise-control feature of PURE, since the integral term k_I^x was non-zero for all mWCUs. The variations of ride sensitivities were more prominent for spinning movements. The standard errors of $k_P^{z,CW}$, $k_P^{z,CCW}$ were 50%-70% of their average values for ABUs and mWCUs, indicating the need for accommodating a wide range of preferences for spinning maneuvers. mWCUs desired asymmetric spinning sensitivities which may be attributed to their permanent spinal disfigurations.

Interestingly, all participants chose the default zero values for k_P^y, k_I^y for translating left/right. This may be due to the natural preference of moving longitudinally over moving laterally due to natural human locomotion behavior and intrinsic non-holonomic design of traditional mWCs [25], [26]. ABUs typically walk forward and turn (but do not move sideways) during locomotion, and traditional mWCs cannot slide. Thus, the ABUs and mWCUs may prefer to have less sensitivity for sideway motions since both groups are more familiar with steering (i.e., translating longitudinally + spinning) than sliding left/right.

There were a few limitations and future work regarding the physical human-robot interface design, controller design, overall test setup, and participant demographics. In terms of hardware, PURE relied on wearable solutions (i.e., IMU) that may not be practical in real-life settings since attaching and detaching the IMU was a tedious task. Also, the IMU sometimes exhibited drifting issues that required re-zeroing of the sensor, causing PURE to spin involuntarily. Non-wearable and drift-free solutions for estimating torso twist angle should be investigated.

A data-driven human-robot interface mapping scheme can be used to automatically tailor PURE's human-robot interface to each rider's preference. While PURE offered many tunable parameters, these parameters utilized a linear mapping scheme based on a univariate model. However, a more personalized mapping scheme may be introduced by utilizing data-driven non-linear and multivariate models [27], [28]. These solutions would autonomously learn the user's preferred strategy to control the robot and provide a more personalized human-robot mapping.

A more realistic test setup can be devised to more accurately assess PURE's performance. The testing protocol included a movable safety gantry and 2D obstacles to minimize the risks of injury. Now that this study has demonstrated PURE's reliability and safety, these safeguards may be removed or replaced since no adverse events or injuries occurred. The safety gantry may be removed to provide more free space for the rider and reduce potential psychological (e.g., fear of colliding with the gantry) or physical (e.g., fitting of safety harness) effects on the rider. We postulate that PURE's performance will improve in real-life settings since the safety harness and gantry system, which could have negatively affected the rider's performance, will not be used in real-life scenarios. Also, the flat obstacles and taped boundaries in this experiment imposed more difficulty because the participants had to look downward periodically to visually perceive the free gap between the taped obstacles and PURE's safety ring. The obstacles can be replaced with 3D obstacles that are easier to visually identify and even physically interact with the objects (e.g., gently touching the wall with hands) to assist with the navigation.

Also, more diverse participant groups should be tested. This study prioritized the participant's safety, so a convenience sample of young and athletic mWCUs were tested. The recruitment of mWCUs was difficult; similar studies tested very few mWCUs (N < 3) [26], [29]. Nevertheless, future studies should test mWCUs who are not para-athletes to determine if PURE could be easily navigated by diverse users. These may include participants with different age, types (e.g., paraplegic, congenital, neuromuscular) and levels (e.g., SCI levels) of disability should be recruited.

5 CONCLUSIONS

A novel hands-free (HF) control that uses the rider's torso motions to maneuver an innovative personal mobility device (PURE) was developed. The ABUs and mWCUs drove PURE using the HF control and joystick (JS) control (a common human-robot interface) through a challenging indoor course in which the performance was assessed in terms of efficiency, efficiency, comfort, and robustness. The HF control performed as well as the JS control for both mWCUs and ABUs. Also, the mWCUs performed as well as the ABUs using the HF and JS control.

ACKNOWLEDGMENTS

We thank the NSF National Robotics Initiative (#2024905), and Yixiang Guo, Chentai Yuan, Eddie Kwon, Patrick Li, and Yintao Zhou for their assistance to the project.

REFERENCES

[1] H. Kaye, T. Kang, and M. Laplante, "Mobility Device Use in the United States," *National Institute on Disability and Rehabilitation Research*, Jun. 2000.

[2] W. E. Pentland and L. T. Twomey, "The weight-bearing upper extremity in women with long term paraplegia," *Spinal Cord*, vol. 29, no. 8, pp. 521–530, 1991, doi: 10.1038/sc.1991.75.
[3] Honda, "Hands-free personal mobility: UNI-ONE." Accessed: Sep. 22, 2023. [Online]. Available: https://global.honda/en/tech/Hands-free_seated_personal_mobility_device_UNI-ONE/
[4] H. G. Nguyen *et al.*, "Segway robotic mobility platform," in *Mobile Robots XVII*, SPIE, 2004, pp. 207–220.
[5] K. Halsall, "Powered mobility device with tilt mechanism having multiple pivots," US9931254B2, Apr. 03, 2015
[6] Scewo, "Scewo Bro." Accessed: Sep. 28, 2023. [Online]. Available: https://www.scewo.com/en/
[7] Genny Mobilitry, "Genny Mobility." Accessed: Sep. 28, 2023. [Online]. Available: https://www.gennymobility.com/en/
[8] C. Xiao, M. Mansouri, D. Lam, J. Ramos, and E. T. Hsiao-Wecksler, "Design and Control of a Ballbot Drivetrain with High Agility, Minimal Footprint, and High Payload," in *IEEE/RSJ International Conference on Intelligent Robots and Systems*, Detroit, Michigan, Oct. 2023.
[9] U. Nagarajan, G. Kantor, and R. Hollis, "The ballbot: An omnidirectional balancing mobile robot," *Int J Rob Res*, vol. 33, no. 6, pp. 917–930, Nov. 2013, doi: 10.1177/0278364913509126.
[10] C. Xiao, "Personal unique rolling experience: Design, modeling, and control of a riding ballbot," Doctoral Dissertation, University of Illinois at Urbana-Champaign, Urbana, 2022.
[11] S. Y. Song *et al.*, "Design and Validation of a Torso-Dynamics Estimation System (TES) for Hands-Free Physical Human-Robot Interaction," in *IEEE Robot and Human Interactive Communication*, Busan, Korea, 2023.
[12] S. Y. Song, N. Marin, C. Xiao, R. Okubo, J. Ramos, and E. Hsiao-Wecksler, "Hands-Free Physical Human-Robot Interaction and Testing for Navigating a Virtual Ballbot," in *IEEE Robot and Human Interactive Communication*, Busan, Korea, 2023.
[13] P. S. Requejo, J. Furumasu, and S. J. Mulroy, "Evidence-Based Strategies for Preserving Mobility for Elderly and Aging Manual Wheelchair Users.," *Top Geriatr Rehabil*, vol. 31, no. 1, pp. 26–41, 2015, doi: 10.1097/TGR.0000000000000042.
[14] "ADA Standards for Accessible Design." Accessed: Sep. 07, 2022. [Online]. Available: https://www.ada.gov/2010ADAstandards_index.htm
[15] S. G. Hart and L. E. Staveland, "Development of NASA-TLX (Task Load Index): Results of empirical and theoretical research," in *Human Mental Workload*, P. A. Hancock and N. Meshkati, Eds., Amsterdam: North Holland Press, 1988, pp. 139–183. doi: 10.1016/S0166-4115(08)62386-9.
[16] R. R. Murphy and D. Schreckenghost, "Survey of metrics for human-robot interaction," in *2013 8th ACM/IEEE International Conference on Human-Robot Interaction (HRI)*, 2013, pp. 197–198. doi: 10.1109/HRI.2013.6483569.
[17] P. Damacharla, A. Y. Javaid, J. J. Gallimore, and V. K. Devabhaktuni, "Common Metrics to Benchmark Human-Machine Teams (HMT): A Review," *IEEE Access*, vol. 6, pp. 38637–38655, 2018.
[18] E. Coronado, T. Kiyokawa, G. A. G. Ricardez, I. G. Ramirez-Alpizar, G. Venture, and N. Yamanobe, "Evaluating quality in human-robot interaction: A systematic search and classification of performance and human-centered factors, measures and metrics towards an industry 5.0," *J Manuf Syst*, vol. 63, pp. 392–410, 2022, doi: https://doi.org/10.1016/j.jmsy.2022.04.007.
[19] A. Steinfeld *et al.*, "Common metrics for human-robot interaction," in *Proceedings of the 1st ACM SIGCHI/SIGART conference on Human-robot interaction*, 2006, pp. 33–40.
[20] J. Accot and S. Zhai, "Performance evaluation of input devices in trajectory-based tasks: an application of the steering law," in *Proceedings of the SIGCHI conference on Human Factors in Computing Systems*, 1999, pp. 466–472.
[21] S. Zhai and R. Woltjer, "Human movement performance in relation to path constraint - the law of steering in locomotion," in *IEEE Virtual Reality, 2003. Proceedings.*, 2003, pp. 149–156. doi: 10.1109/VR.2003.1191133.
[22] J. Accot and S. Zhai, "Beyond Fitts' law: models for trajectory-based HCI tasks," in *Proceedings of the ACM SIGCHI Conference on Human factors in computing systems*, 1997, pp. 295–302.
[23] A. H. Davoudian Talab, A. Badee Nezhad, N. Asadi Darvish, and H. Molaeifar, "Comparison of Anthropometric Dimensions in Healthy and Disabled Individuals," *Jundishapur Journal of Health Sciences (JJHS)*, vol. 9, no. 3, p. e59009, 2017, doi: 10.5812/jjhs.59009.
[24] "Understanding wheelchair sizes and how to ensure it's right for you," Passionate People. [Online]. Available: https://www.passionatepeople.invacare.eu.com/understanding-wheelchair-sizes/
[25] M. A. Hollands, A. E. Patla, and J. N. Vickers, "'Look where you're going!': gaze behaviour associated with maintaining and changing the direction of locomotion.," *Exp Brain Res*, vol. 143, no. 2, pp. 221–230, Mar. 2002, doi: 10.1007/s00221-001-0983-7.
[26] Y. Chen, D. Paez Granados, H. Kadone, and K. Suzuki, "Control Interface for Hands-free Navigation of Standing Mobility Vehicles based on Upper-Body Natural Movements," in *IEEE/RSJ International Conference on Intelligent Robots and Systems (IROS)*, Las Vegas, NV, USA, Oct. 2020, pp. 11322–11329. doi: 10.1109/IROS45743.2020.9340875.
[27] M. Jenifer *et al.*, "Data-driven body–machine interface for the accurate control of drones," *Proceedings of the National Academy of Sciences*, vol. 115, no. 31, pp. 7913–7918, Jul. 2018, doi: 10.1073/pnas.1718648115.
[28] J. Miehlbradt *et al.*, "Data-driven body–machine interface for the accurate control of drones," *Proceedings of the National Academy of Sciences*, vol. 115, p. 201718648, Jul. 2018, doi: 10.1073/pnas.1718648115.
[29] E. B. Thorp *et al.*, "Upper Body-Based Power Wheelchair Control Interface for Individuals With Tetraplegia," *IEEE Trans Neural Syst Rehabil Eng*, vol. 24, no. 2, pp. 249–260, Feb. 2016, doi: 10.1109/TNSRE.2015.2439240.